Decellularization of kidney tissue: Comparison of sodium lauryl ether sulfate and sodium dodecyl sulfate for allotransplantation in rat

Mohammad Amin Keshvari
Bushehr University of Medical Sciences
Alireza Afshar
Bushehr University of Medical Sciences
Sajad Daneshi
Shiraz University of Medical Sciences
Arezoo Khoradmehr
Bushehr University of Medical Sciences
Mandana Baghban
Shiraz University of Medical Sciences
Mahdi Muhaddesi
Bushehr University of Medical Sciences
Pouya Behrouzi
Bushehr University of Medical Sciences
Mohammad Reza Miri
Bushehr University of Medical Sciences
Hossein Azari
Bushehr University of Medical Sciences
Iraj Nabipour
Bushehr University of Medical Sciences
Reza Shirazi
UNSW: University of New South Wales
Mehdi Mahmudpour
Bushehr University of Medical Sciences
Amin Tamadon (amintamaddon@yahoo.com)
Bushehr University of Medical Sciences https://orcid.org/0000-0002-0222-3035

Research Article

Keywords: Decellularized scaffold, Recellularization, Kidney, Rat, Sodium dodecyl sulfate, Sodium lauryl ether sulfate

Posted Date: February 17th, 2021

DOI: https://doi.org/10.21203/rs.3.rs-229858/v1

Abstract

Background: Chronic kidney diseases and end stage renal disease are growing threats worldwide. Tissue engineering is a new hope to surpass the current limitations such as the shortage of donor. To do so, the first step would be fabrication of an intact decellularized kidney scaffold. In the current study, an automatic decellularization device was developed to perfuse and decellularize male rats' kidneys using both sodium lauryl ether sulfate (SLES) and sodium dodecyl sulfate (SDS) and to compare their efficacy in kidney decellularization and post-transplantation angiogenesis.

Methods: After anesthesia, kidneys were perfused with either 1% SDS solution for 4 h or 1% SLES solution for 6 h. The decellularized scaffolds were stained with hematoxylin and eosin, periodic acid Schiff, Masson's trichrome, and Alcian blue to determine cell removal and glycogen, collagen and glycosaminoglycan contents, respectively. Moreover, scanning electron microscopy was performed to evaluate the cell removal and preservation of microarchitecture of both SDS and SLES scaffolds. Additionally, DNA quantification assay was applied for all groups in order to measure residual DNA in the scaffolds and normal kidney. In order to demonstrate biocompatibility and bioactivity of the decellularized scaffolds two tests were done. The scaffolds were recellularized with the human umbilical cord mesenchymal stromal/stem cells (hUC-MSCs). In addition, the allotransplantation was performed in back muscle and angiogenesis was evaluated.

Results: Complete cell removal in both SLES and SDS groups was observed in scanning electron microscopy and DNA quantification assays. Moreover, the extracellular matrix architecture of rat kidney in the SLES group was significantly preserved better than the SDS group. The hUC-MSCs were successfully migrated from the cell culture plate surface into the SDS and SLES decellularized scaffolds. The formation of blood capillaries and vessels were observed in the kidney allotransplantation in both SLES and SDS decellularized kidneys.

Conclusions: We demonstrated that both SLES and SDS could be promising tools in kidney tissue engineering. The better preservation of extracellular matrix than SDS, introduces SLES as the solvent of choice for kidney decellularization.

1. Introduction

The kidney diseases have many diversity and complexity such as acute kidney injury (AKI), chronic kidney disease (CKD) and end-stage renal disease (ESRD) (Romagnani et al. 2017). Recently, following the increased prevalence of non-communicable metabolic diseases such as diabetes mellitus, hypertension and metabolic syndrome, ESRD is a rapidly growing cause for morbidity and mortality worldwide (Romagnani et al. 2017). In order to treat ESRD patients, renal replacement therapy methods such hemodialysis, peritoneal dialysis and renal transplantation have been introduced (Davison and Moss 2016; Gander et al. 2019). These treatments are expensive, time-consuming and not available to the majority of people. The majority of mortalities of ESRD are occurring in the developing countries of

Asia and Africa with low and middle-income, which their people don't have enough accessibility to, or can't afford these treatment modalities (Emem-Chioma et al. 2019). Additionally, the rising number of patients requiring renal replacement therapy alongside the shortage of acceptable donors are concerning issues (Meersch and Zarbock 2018).

To overcome these limitations, tissue engineering has been introduced as a promising new method to treat chronic kidney disease and ESRD patients (Moon et al. 2016). Several *in vitro* and *in vivo* studies in the field of kidney tissue engineering have demonstrated the efficacy of tissue engineering in the treatment of kidney diseases as a new therapeutic approach (Vardar 2020). Alongside with artificial kidney scaffolds, cell- and nucleic acids-free biological scaffolds are new approaches for renal transplantation (Figliuzzi et al. 2017). Using a decellularized kidney scaffold in order to seed patients' own stem cells would be a proper approach to some dilemma in the developing of the engineered kidney (Remuzzi et al. 2017). A crucial step toward for producing a kidney with a natural function is to obtain an acellular kidney scaffold (Li et al. 2016). Therefore, a proper decellularizing agent, which is usually a detergent might be essential, to clean the cells and even their nucleic acids. These methods may provide an extracellular matrix (ECM) including their main proteins, functional and structural molecules which all of them might have an important role in cell filtration, attachment, differentiation and proliferation (He et al. 2017).

There are different decellularizing agents such as sodium dodecyl sulfate (SDS), surfactants, triton X-100, enzymatic and mechanical agents (Gilpin and Yang 2017). The previous study in porcine heart tissue has shown that SDS may potentially damage ECM proteins (Momtahan et al. 2016). In addition, the residue of detergent in a scaffold may induce apoptosis, cellular dysfunction, and thrombosis (Momtahan et al. 2016). Another detergent for decellularization is sodium lauryl ether sulfate (SLES) that have been used to decellularize rat heart (Ma et al. 2018). The SLES is a weaker detergent in comparison to SDS (Emami et al. 2020). To best of our knowledge, there is no decellularizing study on kidney tissue using SLES. Since it has been reported that SLES had good results on heart, lung and bone tissues (Emami et al. 2020; Kawasaki et al. 2015; Ma et al. 2018), and sensitivity and complexity of kidney tissue which is composed of abundant vasculature, it was assumed that SLES might be a better detergent in comparison to SDS in preserving ECM. In the present study, we compared the efficacy of these two detergents (SDS and SLES) for kidney tissue decellularization and their effects on post-transplantation angiogenesis.

2. Materials And Methods

2.1. Animals preparation

This experimental study was approved by Bushehr University of Medical Sciences Ethics Committee (IR.BPUMS.REC.1398.105). Male Sprague-Dawley (200–250 g) were purchased from animal laboratory of Research and Clinical Center for Infertility, Shahid Sadoughi University of Medical Sciences. All animal experiments were performed in Bushehr University of Medical Sciences. The animals were housed under controlled temperature of 23±1°C, 55±5% relative humidity, and 12-hour light/dark cycles. They had free

access to standard food and water during the experimental periods. Rats were randomly divided into three groups: normal group as the control group, SDS group rats were decellularized with SDS, and SLES group rats were decellularized with SLES. In the SDS and SLES groups, rats were used for perfusion studies, histology, electron microscopy, DNA quantification and subcutaneous implantation. The perfusion studies and subcutaneous transplantation were not performed in the normal group.

2.2. Kidney decellularization

At the first, the rats were anesthetized with ketamine (200 mg/kg, Alfasan Co. Netherland) and xylazine (10 mg/kg, Alfasan Co. Netherland). A longitudinal abdominal incision was made and the left kidney, aorta, vena cava and ureter were identified. Heparin (Caspian Tamin Co., Iran) was injected into inferior vena cava to prevent blood clotting during the operation. Renal artery was cannulated and perfused with 0.1 M phosphate buffer saline (PBS) for 2 h at a flow rate of 2 mL/min to remove blood from the kidney using an automatic decellularization system (Percia ADS, PersiaVista R&D Co., Iran) and the renal vein was cut. The detergents, 1% SDS (Parstous Biotech Co., Iran) for 4 h or 1% SLES (Kimia Tehran Acid Co., Iran) for 6 h were perfused at a flow rate of 1 mL/min, separately in each group. Then PBS was perfused another 2 h to remove the remaining detergents in the scaffold. The physiological pressure was maintained within 62 to 107 mmHg (assumed to be rat kidney pressure) by setting the device flow rate between 1 to 2 mL/min through the entire duration of the decellularization process.

2.3. Histological evaluation

The acellular SDS and SLES scaffolds and normal kidneys were fixed in 10% paraformaldehyde, dehydrated using ascending concentration of alcohol, embedded in xylene and paraffin and 5 μm sections were obtained. Hematoxylin and eosin (H&E), Masson's trichrome for collagen detection, Alcian blue for glycosaminoglycans (GAGs) analysis, and periodic acid–Schiff (PAS) for glycogen substances staining were performed with standard protocols (Arenas-Herrera et al. 2013; Liu et al. 2015; Ross et al. 2009). The slices of the SDS and SLES decellularized scaffolds were observed by light microscope (Olympus, Japan) and images captured by phone camera (Samsung A8 2017, Korea) and microscope-phone adaptor (PerciaVista Co., Iran).

2.4. Image analysis

Image analysis was performed by ImageJ software (Fiji-ImageJ x64, US National Institutes of Health). In details, using "Image type" option in "Image" panel, images were converted to 8-bit. Then images scale was set using "Set scale" option in "Analyze" panel. The non-stained area in different staining was selected and measured manually by "Threshold" algorithm. The selected non-stained area of images was calculated by "Analyze particles" option in analyze panel. Finally, the data of non-stained area was extracted from "ROI manager" panel and saved as an excel file with CSV format.

2.5. Scanning electron microscopy (SEM)

SEM was performed based on a method previously used by Kashi et al. (Kashi et al. 2014). Briefly, to assess microarchitecture of acellular scaffolds, the samples were fixed in 2.5% glutaraldehyde for 24 h at 4°C and then dehydrated in an increasingly graded ethanol series (50%, 70%, 90%, and 100%). Then samples were transferred into a 1:2 solutions of hexamethyldisilazane (HMDS) to 100% ethanol then into a 2:1 solution of HMDS to 100% ethanol and finally into a 100% HMDS solution overnight to air-dry in a fume hood, respectively. Finally, samples were covered with a thin layer of gold using Q150R-ES sputter coater (Quorum Technologies, London, UK) and imaged by a VEGA3 microscope (TESCAN, Czech Republic).

2.6. DNA quantification

DNA quantification was performed using a commercial kit (TritaGene Co., Iran). The decellularized scaffold and the normal kidney were sliced into four pieces and one part was weighted and used for the test. At the first step, samples washed with PBS and then were homogenized using ultrasonication method and 750 µL PBS was added to this homogenized solution. The solution was centrifuged for 30 secs at a rate of 9000 rpm. Then the supernatant PBS was removed and care was taken not to scatter and remove the sediment particles. First, 25 µL of cell lysis buffer 1 was added and was vortexed for 30 sec. Then 600 µL of cell lysis buffer 2 was added to the mixture and was vortexed. The solution was centrifuged for 90 secs at a rate of 9000 rpm. The upper portion removed. Then the precipitant was washed with washing solutions. Another centrifuge was performed for 90 secs at a rate of 9000 rpm and then again upper portion of solution was removed. Finally, 40 µL of distilled water was added. The quantity and quality of extracted DNA was measured using nanodrop (DeNovix Co., USA).

2.7. *In vivo* study of decellularized scaffolds

2.7.1. Kidney tissue preparation

The sectioning matrix (Percia Vista Co., Iran) was used to cut the kidney tissues, accurately (Figure S1). The sectioning matrix was printed by fused deposition modeling (FDM) 3D printer (Percia Vista Co., Iran). The polylactide acid (PLA) was used as filament (PLA+, eSUN 3D Co., China) for 3D printing of this sectioning matrix. For 3D printing of sectioning matrix, the “Sectioning_chamber.stl” file which is available on supplementary material of Tyson et al. (Tyson et al. 2015) as a 3D model was used. The Simplify3D software (Simplify3D Co., US) was used to configure and convert the STL file to G-code. The parameter of printing was set as “Auto-Configure for Material” and then was modified manually as described in Table S1. The "Default Printing Speed " in the Simplify3D software was set to 1080mm/min (Figure S2). However, the software automatically adjusted the speeds in different areas to reduce the possibility of failure during printing.

Using this 3D printed sectioning matrix, we were able to cut and prepare the kidney scaffolds with the same size and accuracy. To do so, 11 stainless steel razor blades were used. Firstly, the two blades were placed in the first and the last slit to fix the tissue, and then the other blades were slowly placed in the other slits in order to cut the decellularized kidney scaffolds. Using this 3D printed sectioning matrix, the SDS and SLES decellularized kidney scaffolds were cut separately to same size of 2 mm. There was no rupture in the tissues during sectioning by the 3D printed sectioning matrix. The sliced scaffolds were kept at PBS supplemented with 2 percent penicillin-streptomycin (Pen-Strep) at 4°C in refrigerator.

2.7.2. Kidney recellularization

The human umbilical cord mesenchymal stromal/stem cells (hUC-MSCs) was purchased (Percia Vista Co., Iran). hUC-MSCs were seeded at density of 4×10^5 in 6-well cell culture plate. The culture media was Dulbecco's Modified Eagle Medium (DMEM, Gibco, Life Technologies Co., US) supplemented with 10% fetal bovine serum (FBS, Kiazist Co., Iran) and 1% Pen-Strep (Gibco, Life Technologies Co., US). After 3 days, the cells reached 90 percent confluency. After that, the 2 mm sliced of SDS and SLES decellularized kidney scaffolds were washed 3 times with PBS supplemented with 1% Pen-Strep. The scaffolds were separately explanted in wells of cell-seeded plate. At this stage, the culture media was very low (only covered the cell surface) in order to let the scaffolds attach the bottom of the plates. After 10 min, 2 mL of culture media was added into each well carefully. The 6-well cell culture plate with the attached scaffolds were maintained at incubator with 5% CO_2 and 37°C temperature for 6 days. Additionally, 1 mL of culture media was added into each well at day 3.

2.8. *In vivo* study of decellularized scaffolds

2.8.1. Animal model of transplantation

Six male Sprague-Dawley rats (n=3) with 3-month-old were purchased from the Center of Comparative and Experimental Medicine, Shiraz University of Medical Sciences. They were kept in optimized condition including temperature of 23±2°C, 12h light/dark control and free access to food and water for one week. The rats were housed in separate cages. The cages were cleaned every 5 days. All surgical procedures were performed under general anesthesia by intraperitoneal injection of ketamine-xylazine (1 mg/kg BW 10% ketamine and 0.25 mg/kg BW 2% xylazine). The hair of the back between their shoulders was completely shaved and sterilized by povidone-iodine (Sahand Co., Iran). The skin and fascia were cut about 1 cm in length and then the back muscle was cut using fine watchmakers' forceps to make a hole 3–5-mm deep. The 0.5 cm pieces of each SDS and SLES decellularized scaffolds were used for the SDS and SLES groups, inserted into back muscle and sutured by absorbable sutures (Pezeshkyaran Co., Iran). Finally, the skin was sutured and the animals were kept in standard condition for one month.

2.9. Histological evaluation of recellularized and transplanted scaffolds

After one month, the animals were sacrificed and the SDS and SLES decellularized transplanted scaffolds were separated from muscles and fixed by 10% formaldehyde. The recellularized kidney scaffolds and transplanted scaffolds were separately processed by tissue processor (Didsabz Co., Iran) and paraffin embedded blocks were cut into 7 µm using microtome (Didsabz Co., Iran). Slices were dewaxed and rehydrated in xylene and descending percentage of ethanol (100%, 90%, and 70% ethanol, respectively) and were stained with H&E dye (Arian Cellul Sepehr Co., Iran). Then, the slices were dehydrated by ascending percentage of ethanol and were cleared by xylene. Finally, the slices were mounted by Shandon™ Consul-Mount™ glue (Thermo Fisher Scientific Inc. Germany) and covered by glass coverslip. In the SDS and SLES slices, the angiogenesis and cell infiltration were qualitatively evaluated using light microscope (Olympus, Japan) and images captured by phone camera (Samsung A8 2017, Korea) and microscope-phone adaptor (PerciaVista Co., Iran).

2.9. Statistical analysis

The data were analyzed using IBM SPSS Statistics 26 software (SPSS for Windows, version 26, SPSS Inc, Chicago, Illinois, USA). The statistical analyses were performed using one-way ANOVA and *post hoc* Tukey test. Quantitative data were expressed as the mean value ± standard error of mean (SEM). Additionally, *p* values of less than 0.05 was considered statistically significant. Graphs drawing was performed by GraphPad Prism software (v7.0a, GraphPad Software, Inc., San Diego, CA, USA).

3. Results

3.1. Macroscopically, SLES and SDS decellularized kidney

The scaffolds changed macroscopically during decellularization process. The color of the SDS and SLES kidney scaffolds became pale and finally turned to white and became semi-translucent (Figure 1). The tubules were recognizable in decellularized scaffolds. Total kidney shape was preserved after decellularization procedure without any malformation. Macroscopically, there could be no difference seen between the SDS and SLES kidney scaffolds after decellularization.

3.2. Microscopically, SLES preserved ECM of kidney better than SDS

Histological analysis of the stained tissues showed that cells were successfully removed in both decellularized scaffolds, compared with the normal kidney (Figure 2). Despite of the removing of cells in two scaffolds, the architecture of blood vessels, renal tubules and Bowman capsules were well preserved.

The histological images of the decellularized kidneys showed that the renal tubules structures were more preserved with the SLES than SDS scaffolds (Figure 2). In histological evaluation, the amount of non-stained areas in the SDS and SLES scaffolds with all staining methods were higher than the control kidney, which indicate the decellularization of kidney (p<0.001, Figure 3). The H&E staining of cortex and medulla of rat kidney showed that the SDS and SLES kidney scaffolds had higher percentage of non-stained area than the normal kidney scaffolds (p<0.001, Figure 3A). Moreover, there was a higher percentage of non-stained area in the SDS scaffold than the SLES scaffold in cortex, which was not similar to renal medulla (p<0.001).

The histological image analysis of Masson's trichrome showed a significant higher percentage of non-stained areas in the SDS scaffolds than the SLES scaffolds in kidney cortex (p<0.001, Figure 3B). In other words, the collagen and other ECM fibers in the SLES scaffold was higher than the SDS scaffold. In cortical assessment, the non-stained areas of the SDS and SLES scaffolds were higher than the control kidney, like the H&E staining (p<0.001). In contrast to cortex, in the medulla, the image analysis of Masson's trichrome demonstrated that there was no significant difference between the SDS and SLES scaffolds in non-stained area. In addition, in line with cortex analysis, the non-stained areas of the SDS and SLES scaffolds were higher than the control kidney (p<0.001).

The Alcian blue staining was performed to stain GAGs. The result of image analysis showed that in cortex and medulla of kidney of the scaffolds, the non-stained areas percentage of the SDS and SLES kidney scaffolds were higher than the normal kidney scaffolds (p<0.001, Figure 3C). In cortex, the non-stained area percentage of SDS kidney scaffold was higher than the SLES kidney scaffold (p<0.001), in contrast with the medulla of kidney scaffolds which in there was no significant difference in GAGs amount in the SDS and SLES scaffolds.

Moreover, the PAS staining was used to detect and evaluate the glycogen content of the scaffolds. The PAS staining analysis showed that in both cortex and medulla, the non-stained areas percentage in the SDS and SLES scaffolds were higher than normal scaffold, like the previous staining (p<0.001, Figure 3D).

3.3. The ECM of scaffolds of SLES was better preserved than SDS

The SEM evaluation of normal and decellularized scaffolds showed that the scaffolds were well decellularized (Figure 4A). The microarchitecture of renal tissue scaffolds was well preserved. Furthermore, the three-dimensional spaces of cleared various cells remained unscathed. Additionally, in higher magnification, the ECM structure was appeared to be intact (Figure 4B). The structure and direction of scaffold’s fibers like collagen was also intact. In addition, the microarchitecture integrity of tissue in the SDS scaffolds was lesser than the SLES scaffolds (Figure 4).

3.4. SLES and SDS removed the DNA content of the kidney scaffolds

The DNA content of normal kidney (149.8 ± 54.2 ng/mg of dry tissue weight) was higher than the SDS and SLES scaffolds ($p<0.05$, Figure 4C). Moreover, the DNA evaluation of the scaffolds revealed that the DNA content of the SLES scaffolds was zero (0 ng/mg of dry tissue weight). Although there was no significant difference between the DNA content of the SDS and SLES scaffolds ($p>0.05$), the DNA content of the SDS scaffolds was not zero (1.2 ± 0.2 ng/mg of dry tissue weight).

3.5. SLES and SDS scaffolds were recellularized by hUC-MSCs

The hUC-MSCs were successfully migrated from the cell culture plate surface into the SDS and SLES decellularized scaffolds. The cells were flattened and attached to both scaffolds structure (Figures 5A and 5B). This result suggested that the decellularized rat scaffolds were compatible to human cells and they were viable and adherent. In addition, the number of cells migrated to scaffolds in SLES decellularized scaffolds was not significantly different with the SDS decellularized scaffolds (Figure 5C).

3.6. SLES and SDS scaffolds were vascularized after allotransplantation

The SDS and SLES kidney scaffolds showed bioactivity and biocompatibility after allotransplantation in the rat back muscle. There was no scaffold rejection in the SDS and SLES scaffolds after the scaffolds allotransplantation. Additionally, there was no toxic effect of scaffolds on recipient body. After one month of scaffolds' transplantation, the transplanted the SDS and SLES scaffolds were evaluated. Although there was no evidence of rejection in the grafts, there was scarce infiltration of host cell into the grafts which some of them were leukocytes (Figure 6). Moreover, the angiogenesis process was evaluated after one month of the SDS and SLES scaffold transplantation. The H&E staining revealed that new vascularization was taken place in the SDS and SLES scaffolds (Figure 6). The vascular tubular shape and red blood cells inside of these tubules indicated the neovascularization. In the SDS and SLES scaffolds, three types of vessels were observed; large vessels, small vessels, and very small vessels (arterioles or capillaries) (Figure 6). The very small vessels were distinguished from other vessels by their narrowing and the thin layer of their walls (Figure 6). The number of large vessels in the SDS and SLES scaffolds was qualitatively determined which was between 0 to 2 vessels per each field. Additionally, the number of small vessels was counted which was between 2 to 5 vessels per each field, and number of very small vessels was counted which was between 1 to 5 vessels per each field.

4. Discussion

Kidney tissue engineering is an emerging technology in regenerative medicine which has been targeted to overcome the kidney donation limitations for renal transplantation. To do so, at the first step, a proper scaffold needed for transplantation. The present study was conducted to decellularize kidney and finally produce a proper scaffold in rats. In decellularization procedure, especially in the vessels, an important part is the avoidance of clot formation (Simsa et al. 2018; Walawalkar and Almelkar 2019). As the kidney has very small vessels, especially arterioles and capillaries, even a small clot can obstruct vessels and impair its blood flow (Geltzeiler and Schwartz 1984). Hence, obstruction of the liquid flow can interrupt the decellularization and cause partial decellularization; therefore, the first step in the present study targeted to prevent clot formation. Therefore, instantly after rat thoracotomy, heparin was injected to the inferior *vena cava.* Then in order to eliminate all blood cells, the tissue was perfused by PBS. After 2 h, the flow liquid which exited from the tissue turned from red into colorless, indicating red blood cells (RBCs) elimination. At the next step, the main decellularization step was performed. Other important aspects of decellularization procedure include the flow rate of decellularization and the percentage of detergents, which were different from each other in different studies (Emami et al. 2020; Hassanpour et al. 2018; He et al. 2017; Nakayama et al. 2010). Based on previous studies and also based on our pilot study, the flow rate and the percent of detergent were optimized. Then, the decellularization process was performed.

The kidney tissues successfully decellularized by SDS and SLES detergents and then, these detergents were compared to the normal kidney tissue. In several studies mammalian tissues were decellularized using SDS detergent with good results (He et al. 2017; Nakayama et al. 2010; Remuzzi et al. 2017). In the present study, the concentration of 1% SDS solution was used, like the previous studies (Nakayama et al. 2010; Remuzzi et al. 2017). The SDS decellularization method had very good results in previous study of tissue decellularization (He et al. 2017; Nakayama et al. 2010; Remuzzi et al. 2017). In recent years, the SLES reagent was also used for tissue decellularization (Emami et al. 2020; Hassanpour et al. 2018; Naeem et al. 2019). This new detergent had very good efficacy for tissue decellularization (Emami et al. 2020; Hassanpour et al. 2018). In order to compare SDS and SLES detergents for kidney decellularization, this study was performed. Firstly, the histological and image analysis was evaluated. The results of histological and image analysis showed that the SDS and SLES scaffolds had higher non-stained areas than the normal kidney, indicating decellularization process. The H&E staining demonstrated that no cells were remained in the SDS and SLES decellularized scaffolds. Additionally, Masson's trichrome staining showed that non-stained areas of the SDS and SLES scaffolds were 82.6 ± 0.7% and 78.2 ± 0.7%, respectively which were higher than the normal kidney counterparts (26.1 ± 0.6%). This indicates that total number of proteins including collagen were reduced in both decellularized scaffolds, however they were not completely deleted.

Furthermore, the Masson's trichrome histology images showed that the structure of kidney scaffolds was preserved after decellularization. This indicates that the total protein structure of kidney in the SDS and SLES scaffolds was preserved. Moreover, two decellularizing agents, SDS and SLES, are comparable with each other. In cortex of the kidney scaffolds, there was significant difference between non-stained areas of the SDS and SLES kidney scaffolds in both H&E and Masson's trichrome staining. These results demonstrate that in SLES scaffolds, the non-stained area was lower than the SDS scaffolds, indicating

that more collagen was preserved in the SLES scaffolds than the SDS scaffolds. This finding may present better effect of SLES detergent in comparison to SDS detergent. In contrast, in medulla, the percentage of non-stained areas in the SLES and SDS scaffolds showed no difference.

The histology of Alcian blue staining showed that the non-stained areas of the SDS and SLES scaffolds were higher than the normal kidney. As the Alcian blue staining represents the content of GAGs and carbohydrates of tissue, such as mucosubstances (Batko et al. 2019), this result showed that most of the GAGs was removed during decellularization process; however, the amounts of GAGs didn't reached zero and some amount of GAGs were preserved in total structure of renal tissue. In addition, the GAGs' amount of the SLES scaffold in cortex was higher than the SDS scaffold which represents that more GAGs in the SLES scaffolds were preserved; indicating another proof for better yield of SLES detergent than SDS. This difference was not observed in medulla of decellularized scaffolds, like the previous staining methods.

Furthermore, the PAS staining of kidney tissues demonstrated that the glycogen substances of the SDS and SLES scaffolds were lower than the normal kidney. This indicates that the total amounts of glycogen were decreased after decellularization and most of them were removed by SDS and SLES detergents; however, the essential parts of them which exist in structural parts of kidney were preserved. Like the previous staining methods, the amount of non-stained area of the SLES scaffold was lower than the SDS scaffold in cortex of kidney scaffolds, indicating that more glycogen in the SLES scaffolds were preserved.

The findings of histological analysis of decellularized kidney showed that SDS and SLES successfully decellularized kidneys. Besides of decellularization, a key element of proper producing of scaffolds is their ECM molecules such as proteins like collagen and elastin, carbohydrates and GAGs (Emami et al. 2020). During decellularization of kidney by SDS and SLES detergents, some of these ECMs factors were removed either. According to the histological analysis, some amount of the ECMs factors were not totally eliminated and total structure of kidney was preserved. Additionally, glomerular and tubular basement membranes were well preserved in the histological staining. In line with the findings of the present study, previous study of SDS and SLES decellularization also demonstrated that the total amounts of ECMs factors reduced after decellularization, but the total structure of tissue and some of these ECMs factors remained intact (Ma et al. 2018). Additionally, the results of current study showed that in some cases, especially in cortex of the SLES scaffolds, the ECM was preserved better. The results of previous studies are in line with the current study and all of them indicates that SLES had better performance in tissue decellularization than SDS reagent (Emami et al. 2020; Ma et al. 2018).

In order to prove the preservation of total structures of decellularized kidney, SEM analysis was performed. The SEM analysis showed that the microstructure of the SDS and SLES scaffolds were well preserved. Furthermore, the pores and three-dimensional spaces of previous cells of kidneys were preserved as well. In higher magnification, it was shown that total structure of ECMs' fibers of SLES scaffolds were more intact than SDS scaffolds. These fibers in the SLES scaffolds were more in line with each other than the SDS scaffolds and the total microstructure integrity of the SLES scaffolds were more

preserved. In consistent with our results, a decellularization study of lung tissue demonstrated a better preservation of the SLES lung scaffolds microstructures than the SDS scaffolds (Ma et al. 2018).

The confirmatory assessment of total decellularization was performed by DNA quantification. The contents of DNA in the SLES scaffolds which was determined by DNA quantification was zero. Furthermore, the DNA contents of the SDS scaffolds were reduced, but not completely eliminated. Additionally, there was no significant difference between the DNA contents of the SLES and SDS scaffolds. However, the DNA contents of the SLES and SDS scaffolds were significantly differ from the normal kidney. These results showed that no nuclei were remained in the SLES scaffolds and these nuclei also reduced remarkably in the SDS scaffolds. Previous studies of tissue decellularization are in line with the results of the present study and they also demonstrated a reduction of total content of DNA after decellularization (Hassanpour et al. 2018; Ma et al. 2018; Sullivan et al. 2012). However, to best of our knowledge, there is no study in literature to show that the DNA content of the SLES scaffolds totally eliminated and reached to zero level.

When the decellularization was confirmed, the biocompatibility and bioactivity of the SDS and SLES scaffolds evaluated in *in vitro* and *in vivo* study. At *in vitro* study, cell migration and scaffold bio-compatibility were analyzed. The hUC-MSCs were successfully migrated into both SDS and SLES scaffolds and no contamination was observed. After that the *in vitro* cell migration and cell bio-compatibility was successfully performed, the *in vivo* analysis started. At the *in vivo* analysis, firstly, no rejection happened after allotransplantation in all recipient rats, indicating biocompatibility of decellularized scaffolds by SDS and SLES. After one month of the transplantation, the scaffolds were evaluated qualitatively by light microscopy. The primary observation showed infiltration of the host cells into the decellularized grafts, which implies their bioactivity. However, in further evaluation, the angiogenesis was observed in the transplanted scaffolds. The vessels were recognized by their tubular shape and the presence of RBCs inside of these tubules. Additionally, most of these vessels had a layer of epithelial cells and in some cases muscular cells around them. The dimeter of these tubules and also the dimeter of layer around them were different. Based on these differences, the vessels divided into three groups; large vessels, small vessels and very small vessels including arterioles and capillaries. Totally, in the qualitative analysis, there was no significant difference between both scaffolds in their angiogenesis. In previous study of rat lung decellularization by SDS and SLES, the similar results of the current study has been shown with a higher amount of infiltrating cells and larger vessels in the SLES scaffolds in comparison to the SDS scaffolds (Ma et al. 2018). These findings may be related to vigorous detergent effect of SDS which makes more depletion of growth factors in the scaffolds (Papalamprou et al. 2016).

5. Conclusions

Taken together, SLES detergent, as a new anionic detergent had a better performance for renal tissue decellularization. To best of our knowledge, this was the first kidney decellularization study which compared and optimized SDS and SLES detergents. The results demonstrated that the rat kidney tissue was entirely decellularized by SDS and SLES. However, the microarchitecture of the scaffolds remained

intact and SLES was more efficient in this preservation process. Additionally, to best of our knowledge, this is the first *in vivo* analysis of the SDS and SLES decellularized kidney scaffolds which evaluated their biocompatibility and bioactivity in an *in vivo* model. The SDS and SLES scaffolds showed angiogenesis and there was no rejection of the SDS and SLES grafts. SLES is a promising detergent that could be a useful decellularization agent to produce acellular kidney scaffold much alike normal kidney scaffold. SLES detergent in comparison with SDS as a strong anionic detergent with higher biodegradation ability, had milder chemical properties and better preservation of ECM proteins and microarchitecture, the properties which later would be crucial for the cell seeding. In summary, SLES is an alternative detergent for SDS which can be used in renal tissue engineering confronting disadvantages related to SDS.

Abbreviations

AKI, acute kidney injury

CKD, chronic kidney disease

DMEM, Dulbecco's Modified Eagle Medium

ECM, extracellular matrix

ESRD, end-stage renal disease

FBS, fetal bovine serum

FDM, fused deposition modeling

GAGs, glycosaminoglycans

H&E, hematoxylin and eosin

HMDS, hexamethyldisilazane

hUC-MSCs, human umbilical cord mesenchymal stromal/stem cells

PAS, periodic acid–Schiff

PBS, phosphate buffer saline

Pen-Strep, penicillin-streptomycin

PLA, polylactide acid

RBC, red blood cells

SDS, sodium dodecyl sulfate

SEM, scanning electron microscopy

SEM, standard error of mean

SLES, sodium lauryl ether sulfate

Declarations

Ethics approval and consent to participate

This experimental study was approved by Bushehr University of Medical Sciences Ethics Committee (IR.BPUMS.REC.1398.105).

Consent for publication

Not applicable.

Availability of data and material

Data are available as requested.

Funding

The authors disclose financial support for the research from the Bushehr University of Medical Sciences (grant no. 1279).

Competing interests

Author Alireza Afshar, Mahdi Muhaddesi and Pouya Behrouzi were employed by the Percia Vista Biotechnology Company. The remaining authors declare that the research was conducted in the absence of any commercial or financial relationships that could be construed as a potential conflict of interest.

Authors' contributions

A.T., R.S., M.M. and I.N. conceived and designed the study. M.A.K., A.A, S.D., A.K., M.B., M.M., M.R.M., H.A., and P.B. collected data and analyzed the findings. M.A.K., A.A, S.D., A.K., and M.B. drafted and edited the manuscript. A.T., R.S., M.M. and I.N. reviewed the manuscript. All authors contributed to the critical reading and discussion of the manuscript. All authors have read and agreed to the published version of the manuscript.

Acknowledgments

The authors wish to thank Clinical Center for Infertility, Shahid Sadoughi University of Medical Sciences; The Center of Marine Comparative and Experimental Medicine, The Persian Gulf Biomedical Sciences Research Institute, Bushehr University of Medical Sciences; and Shiraz University of Medical Sciences for providing lab equipment in this project.

References

Arenas-Herrera J, Ko I, Atala A, Yoo J (2013) Decellularization for whole organ bioengineering Biomed Mater 8:014106

Batko K et al. (2019) Proteoglycan/glycosaminoglycan and collagen content in the arterial wall of patients with end-stage renal disease: new indicators of vascular disease Pol Arch Intern Med 129:781-789

Davison SN, Moss AH (2016) Supportive care: meeting the needs of patients with advanced chronic kidney disease Clin J Am Soc Nephrol 11:1879-1880

Emami A, Talaei-Khozani T, Vojdani Z, Zarei Fard N (2020) Comparative assessment of the efficiency of various decellularization agents for bone tissue engineering J Biomed Mater Res B Appl Biomater

Emem-Chioma P, Wokoma F, David-West M (2019) Community focused primary prevention of risk factors of Chronic kidney diseases (CKD): an unmet need in reducing the burden of ESRD in Low and middle income countries (LIMC) countries-a review and proposition Trop J Nephrol 14:67-88

Figliuzzi M, Bonandrini B, Remuzzi A (2017) Decellularized kidney matrix as functional material for whole organ tissue engineering J Appl Biomater Funct Mater 15:e326-e333

Gander JC et al. (2019) Association between dialysis facility ownership and access to kidney transplantation JAMA 322:957-973

Geltzeiler J, Schwartz D (1984) Obstruction of solitary kidney due to epsilon-aminocaproic-acid-induced fibrin clot formation Urology 24:64-66

Gilpin A, Yang Y (2017) Decellularization strategies for regenerative medicine: from processing techniques to applications Biomed Res Int 2017

Hassanpour A, Talaei-Khozani T, Kargar-Abarghouei E, Razban V, Vojdani Z (2018) Decellularized human ovarian scaffold based on a sodium lauryl ester sulfate (SLES)-treated protocol, as a natural three-dimensional scaffold for construction of bioengineered ovaries Stem Cell Res Ther 9:252

He M, Callanan A, Lagaras K, Steele J, Stevens M (2017) Optimization of SDS exposure on preservation of ECM characteristics in whole organ decellularization of rat kidneys J Biomed Mater Res Part B Appl

Biomater 105:1352-1360

Kashi AM et al. (2014) How to prepare biological samples and live tissues for scanning electron microscopy (SEM) Galen Med J 3:63-80

Kawasaki T et al. (2015) Novel detergent for whole organ tissue engineering J Biomed Mater Res A 103:3364-3373

Li Q et al. (2016) Proteomic analysis of naturally-sourced biological scaffolds Biomaterials 75:37-46

Liu R, Gao J, Yang Y, Zeng W (2015) Preparation of rat whole-kidney acellular matrix via peristaltic pump Urol J 12:2457-2461

Ma J, Ju Z, Yu J, Qiao Y, Hou C, Wang C, Hei F (2018) Decellularized rat lung scaffolds using sodium lauryl ether sulfate for tissue engineering ASAIO J 64:406-414

Meersch M, Zarbock A (2018) Renal replacement therapy in critically ill patients: who, when, why, and how Curr Opin Anaesthesiol 31:151-157

Momtahan N et al. (2016) Using hemolysis as a novel method for assessment of cytotoxicity and blood compatibility of decellularized heart tissues ASAIO J 62:340-348

Moon KH, Ko IK, Yoo JJ, Atala A (2016) Kidney diseases and tissue engineering Methods 99:112-119

Naeem EM et al. (2019) Decellularized liver transplant could be recellularized in rat partial hepatectomy model J Biomed Mater Res A 107:2576-2588

Nakayama KH, Batchelder CA, Lee CI, Tarantal AF (2010) Decellularized rhesus monkey kidney as a three-dimensional scaffold for renal tissue engineering Tissue Eng Part A 16:2207-2216

Papalamprou A, Chang CW, Vapniarsky N, Clark A, Walker N, Griffiths LG (2016) Xenogeneic cardiac extracellular matrix scaffolds with or without seeded mesenchymal stem cells exhibit distinct in vivo immunosuppressive and regenerative properties Acta Biomater 45:155-168

Remuzzi A et al. (2017) Experimental evaluation of kidney regeneration by organ scaffold recellularization Sci Rep 7:43502

Romagnani P et al. (2017) Chronic kidney disease Nat Rev Dis 3:17088

Ross EA et al. (2009) Embryonic stem cells proliferate and differentiate when seeded into kidney scaffolds J Am Soc Nephrol 20:2338-2347

Simsa R et al. (2018) Systematic in vitro comparison of decellularization protocols for blood vessels Plos One 13:e0209269

Sullivan DC, Mirmalek-Sani S-H, Deegan DB, Baptista PM, Aboushwareb T, Atala A, Yoo JJ (2012) Decellularization methods of porcine kidneys for whole organ engineering using a high-throughput system Biomaterials 33:7756-7764

Tyson AL, Hilton ST, Andreae LC (2015) Rapid, simple and inexpensive production of custom 3D printed equipment for large-volume fluorescence microscopy International journal of pharmaceutics 494:651-656

Vardar E (2020) Tissue engineering in urology. In: Biomaterials for Organ and Tissue Regeneration. Elsevier, pp 441-455

Walawalkar S, Almelkar S (2019) Fabrication of aortic bioprosthesis by decellularization, fibrin glue coating and re-endothelization: a cell scaffold approach Prog Biomater 8:197-210

Figures

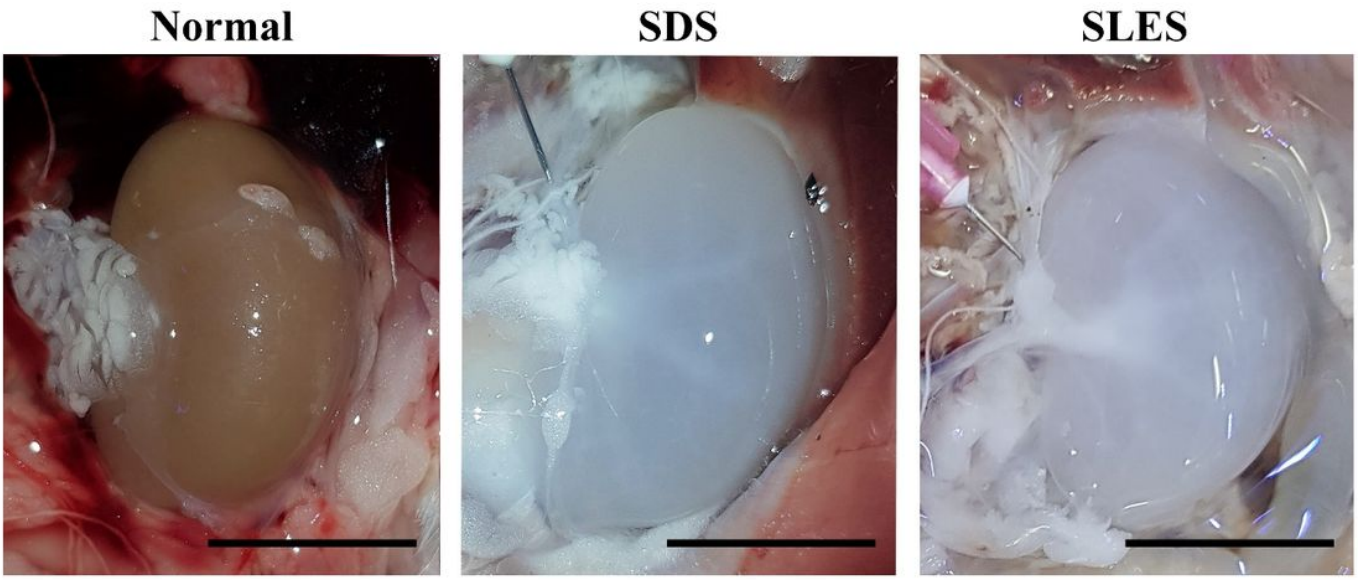

Figure 1

Macroscopic imaging of kidney tissue and decellularized scaffolds using sodium dodecyl sulfate (SDS) and sodium lauryl ether sulfate (SLES) in rat. Scale bars are 1 cm.

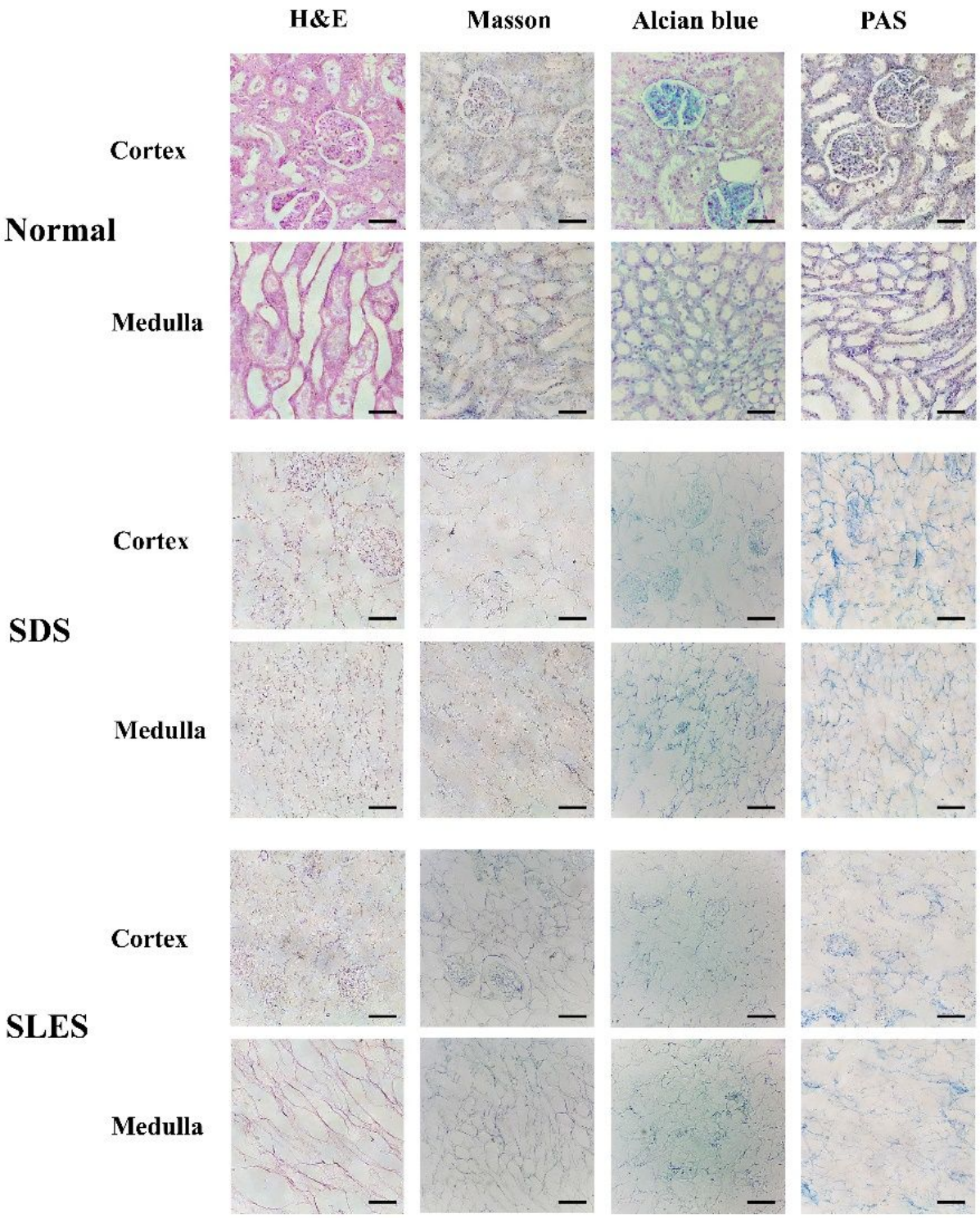

Figure 2

Histologic images of normal kidney and decellularized kidney using sodium dodecyl sulfate (SDS) and sodium lauryl ether sulfate (SLES) in rat. Hematoxylin and eosin (H&E), Masson's trichrome for collagen analysis (Masson), Alcian blue for glycosaminoglycans (GAGs) detection, periodic acid–Schiff (PAS) for glycogen substances staining were performed. Scale bars are 50 μm.

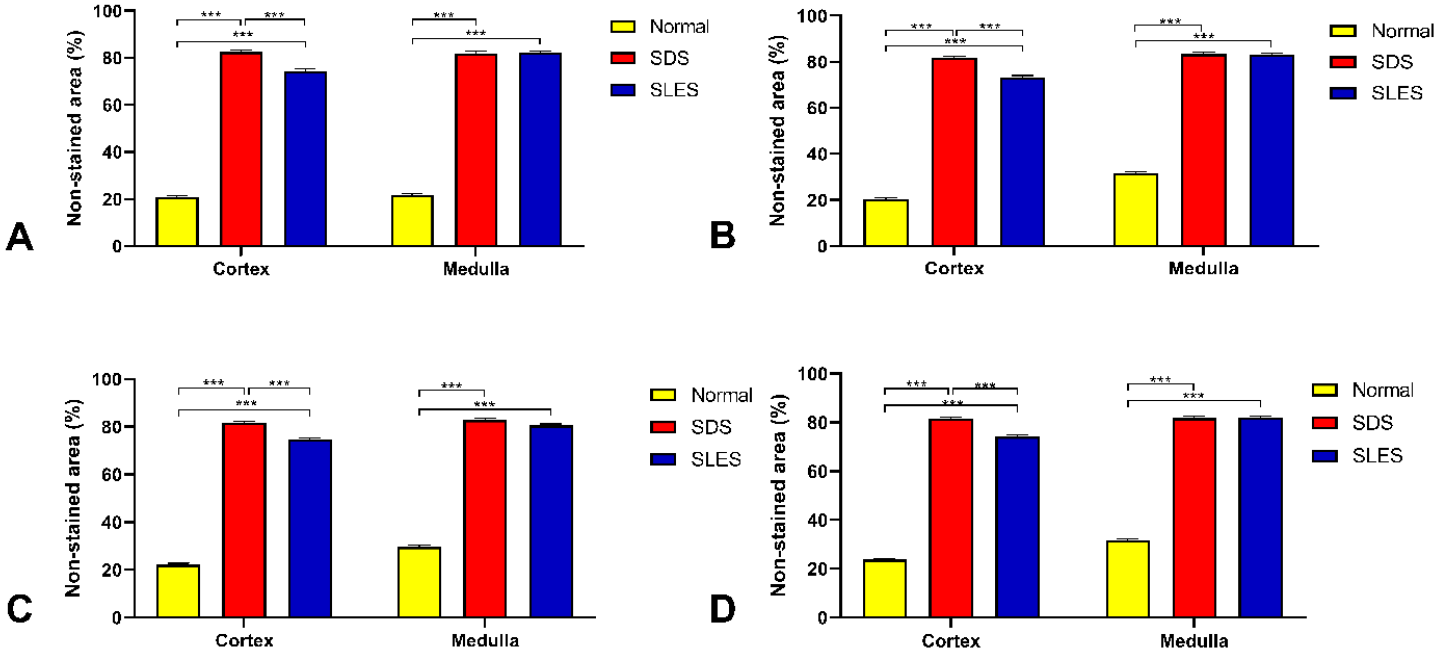

Figure 3

Histologic analysis of normal kidney and decellularized kidney using sodium dodecyl sulfate (SDS) and sodium lauryl ether sulfate (SLES) in rat. A) Image analysis of hematoxylin and eosin staining. B) Image analysis of Masson's trichrome staining. C) Image analysis of Alcian blue staining. D) Image analysis of periodic acid–Schiff (PAS) staining. Lines above the columns show significant differences between the groups (***p<0.001).

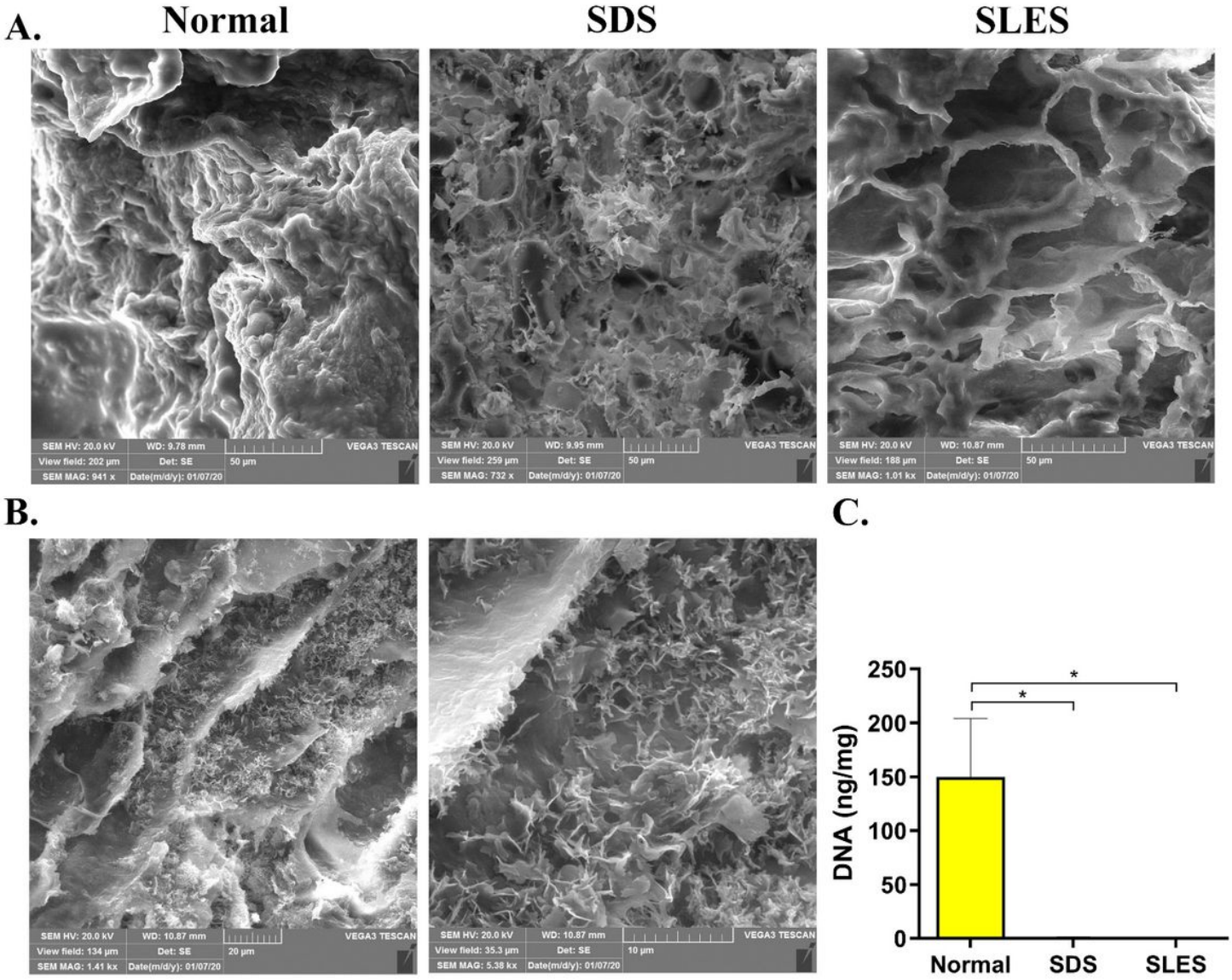

Figure 4

Scanning electron microscopy and DNA quantification analysis of normal kidney and decellularized kidney using sodium dodecyl sulfate (SDS) and sodium lauryl ether sulfate (SLES) in rat. A) Scanning electron microscopy of normal, SDS and SLES kidney scaffolds with 50 nm magnification. B) Decellularized SLES scaffold at higher magnification of 20 and 10 nm. C) DNA quantification of intact kidney and SDS- and SLES-decellularized kidney scaffolds. Lines above the columns show significant differences between the groups (*$p<0.05$).

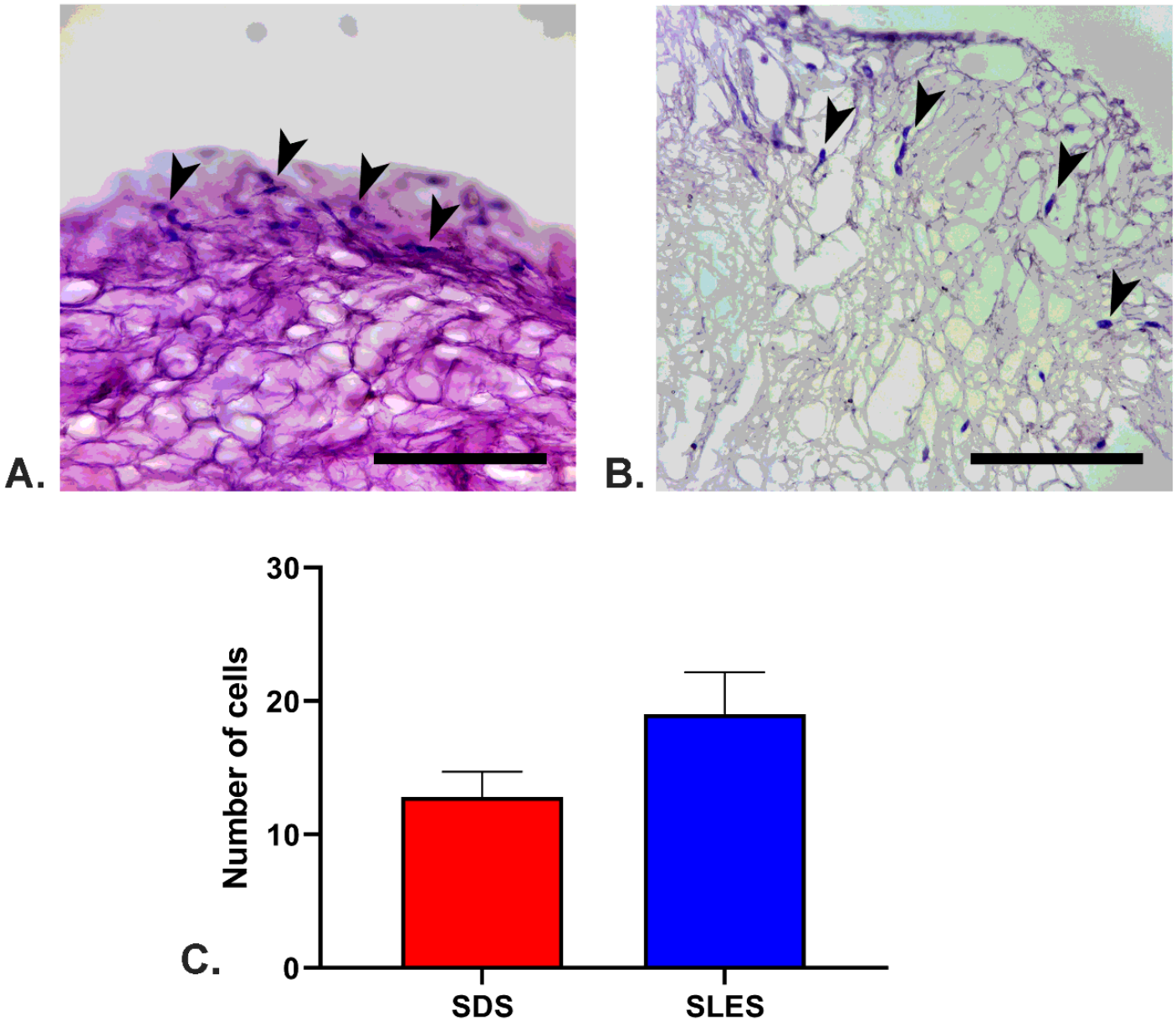

Figure 5

Kidney recellularization. A) Histology of SLES recellularized kidney scaffolds. B) Histology of SDS recellularized kidney scaffolds. C) Number of cells migrated into SDS and SLES kidney scaffolds. Arrow head indicated the HUC-MSCs migrated into scaffolds. The scale bars in bow images are 50 μm.

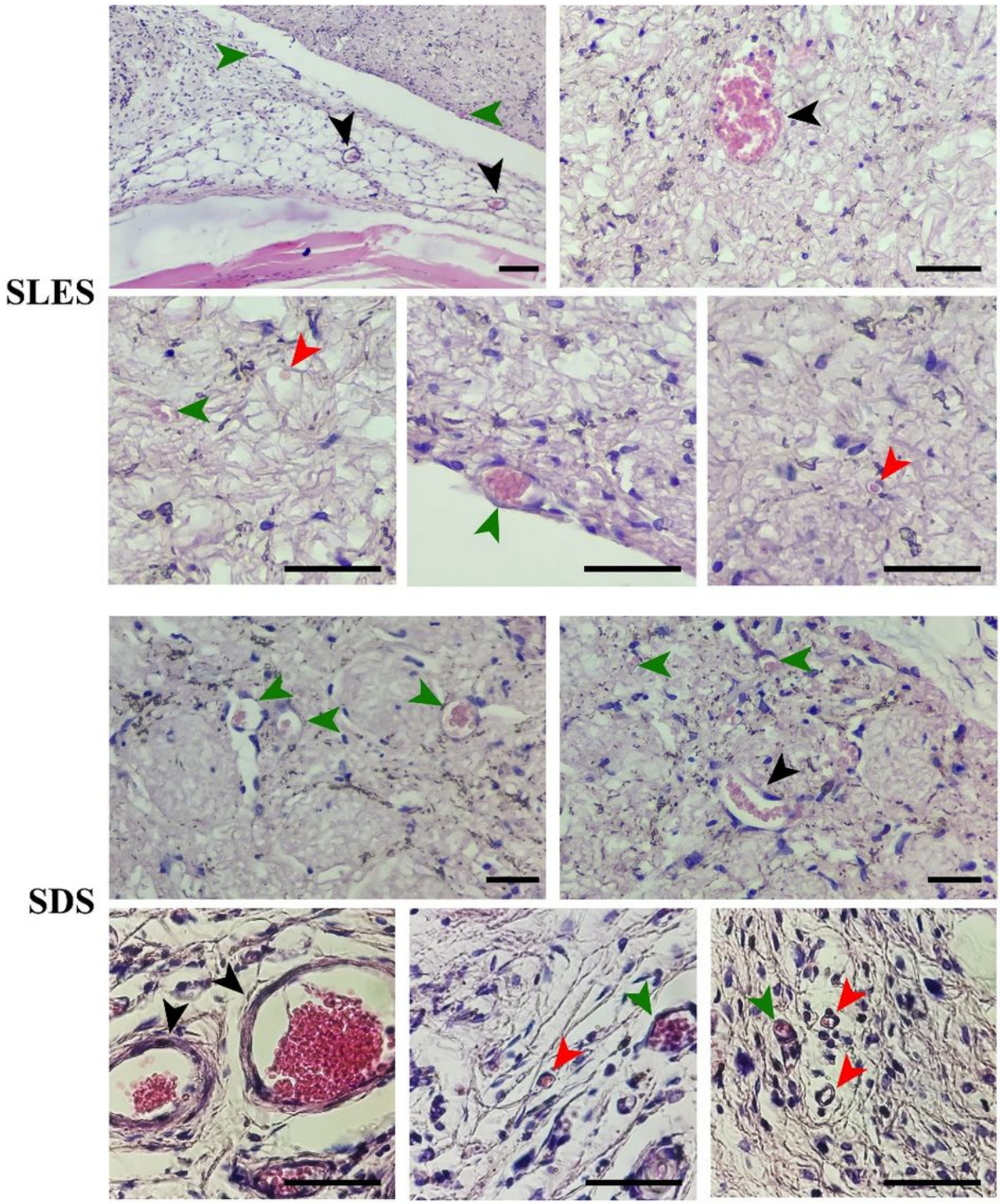

Figure 6

Post-allotransplantation vascularization of kidney scaffolds after decellularization using sodium dodecyl sulfate (SDS) and sodium lauryl ether sulfate (SLES) in rat after 1 month. Angiogenesis and cell infiltration form recipient body has been showed. The black arrows represent large vessels, the green arrows represent small vessels and the red arrows are very small vessels (arterioles and capillaries). The scale bars in all images are 50 μm.

Supplementary Files

This is a list of supplementary files associated with this preprint. Click to download.

- Supplementaryfile.docx